Polymer Chemistry

Accepted Manuscript

ROYAL SOCIETY OF CHEMISTRY

www.rsc.org/polymers

Journal Name

RSCPublishing

ARTICLE

Dynamic intracellular delivery of antibiotics via pH-responsive polymersomes

Cite this: DOI: 10.1039/x0xx00000x

D.D. Lane[1], F.Y. Su[1], D.Y. Chiu, S. Srinivasan, J.T. Wilson, D.M. Ratner, P.S. Stayton, and A.J. Convertine*

Received ooth January 2012,
Accepted ooth January 2012

DOI: 10.1039/x0xx00000x

www.rsc.org/

Reversible addition-fragmentation chain transfer (RAFT) polymerization was employed to prepare a series of copolymers consisting of 2-hdroxyethyl methacrylate (HEMA) and poly(ethylene glycol) methyl ether methacrylate (FW_{avg} ~ 950 Da) (O950) with variable comonomer compositions and molecular weights for use as polymeric scaffolds. Reactivity ratios for the monomer pair were determined to be 1.37 and 0.290 respectively. To these scaffolds trithiocarbonate-based RAFT chain transfer agents (CTAs) were grafted using carbodiimide chemistry. The resultant graft chain transfer agents (gCTA) were subsequently employed to polymerize dimethylaminoethyl methacrylate (DMAEMA) and (HPMA) between degrees of polymerization (DP) of 25 and 200. Kinetic analysis for the polymerization of DMAEMA targeting a DP of 100 from a 34 arm graft gCTA show linear M_n conversion and pseudo first order rate plots with narrow molecular weight distributions that move toward lower elution volumes with monomer conversion. Đ values for these polymerizations remain low at around 1.20 at monomer conversions as high as 70 %. pH-responsive endosomalytic brushes capable of spontaneously self-assembling into polymersomes were synthesized and a combination of dynamic light scattering (DLS), cryoTEM, and red blood cell hemolysis were employed to evaluate the aqueous solution properties of the polymeric brush as a function of pH. Successful encapsulation of ceftazidime and pH-dependent drug release properties were confirmed by HPLC. Intracellular antibiotic activity of the drug-loaded polymersomes was confirmed in macrophage coculture model of infection with B. thailandensis and RAW 264.7 cells.

Introduction

The dissemination of infectious aerosols is considered the most dangerous method of delivering biological weapons.[1] *Francisella tularensis* and *Burkholderia pseudomallei*, the agents of tularemia and melioidosis, respectively, are among the CDC Tier 1 select agents because they present the greatest risk of mass casualties or devastating effects to the economy, critical infrastructure, and public confidence. In the 1990s, biological threat agents (BTAs) and chemical threat agents reemerged as potential weapons of mass destruction with the discovery of agent stockpiles in Iraq as well as ongoing efforts in the former Soviet Union involving genetic engineering of BTAs, novel product development, and large scale manufacturing. Both *F. tularensis* and *B. pseudomallei* are environmentally stable, can be transmitted by aerosol, and can cause a rapid onset of severe illness.[1-3] Because most biothreat agents are designed for aerosol delivery, the lungs are the first target organ, and within the alveoli, the pulmonary macrophage represents the first line of defense against invasion. Both *Francisella tularensis and Burkholderia sp.* have the capability to reside and multiply within macrophages, where they are protected from an adaptive immune response and are more resistant to antibiotics. In spite of advances in the development of new antibiotics, infections caused by these bacteria remain difficult to treat, and pretreatments (e.g., vaccines) are not currently available. Rapid diagnostic tests for tularemia and melioidosis are not readily available, and thus there is a critical need for rapid prophylactic/treatment methods because even effective antibiotics do not prevent disabling illness when treatment is started after the onset of symptoms. The intracellular compartmentalization of these pathogenic organisms within alveolar macrophages is a significant barrier to bacterial clearance and contributes to their associated morbidity and mortality.

Lipids and polymers have been employed extensively to build nanoparticles such as micelles, liposomes, and polymersomes for the controlled delivery of both hydrophilic and hydrophobic drugs.[13,14] These systems can substantially improve the bioavalibility and pharmacokinetic properties of the encapsulated drugs and are capable of integrating other important functional components such as cell-specific targeting

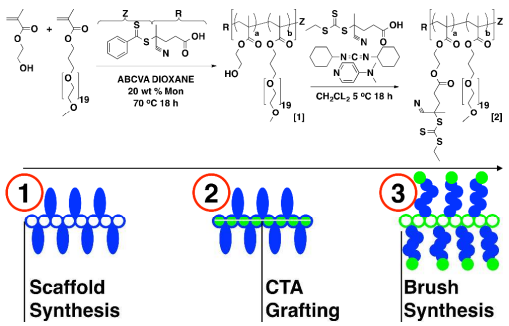

Scheme 1. Synthetic scheme for the preparation of hydroxyl function polymeric scaffolds and subsequent polyfunctional graft chain transfer agents (gCTAs). Copolymerizations of HEMA and O950 were conducted in dioxane over a range of $[M]_o/[CTA]_o$ and between 13 and 100 at a fixed $[CTA]_o/[I]_o$ ratio of 10:1. Carbodiimide coupling of ECT to the hydroxyl-functional scaffolds was accomplished via carbodiimide chemistry in methylene chloride using an initial ratio DCC, DMAP, and ECT to polymeric hydroxyl group of 2:1 at an initial polymer concentration of 10 wt. %. The resultant gCTA was subsequently isolated by repeated precipitation from acetone into ether.

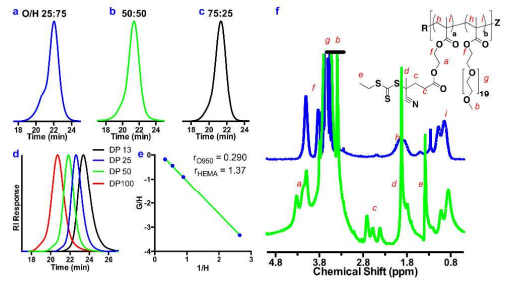

Fig. 1. Characterization of copolymers containing HEMA and O950 prepared by RAFT over a range of initial comonomer compositions and target degrees of polymerization. Molecular weight distribution for copolymers of HEMA and O950 at an initial HEMA and O950 mole percentages of (a) 75:25 (b) 50:50, and (c) 25:75. Molecular weight and Đ values for these copolymers are 15 800/1.07, 20 400/1.08, and 28 000/1.18 respectively. (d) Molecular weight distributions for the RAFT copolymerization of HEMA and O950 conducted at initial $[M]_o/[CTA]_o$ ratios of 13, 25, 50, and 100 at a fixed initial $[M]_o$ and $[CTA]_o/[I]_o$ ratio 20 wt. % and 10 respectively. (e) Inverted Fineman-Ross plot for a series of HEMA and O950 copolymerizations. Copolymerizations were conducted over a wide range of comonomer compositions while maintaining low monomer conversion ($p < 5$ %). (e) 500 MHz ^{1}H NMR data showing conjugation of ECT to polymeric scaffolds. Poly($HEMA_{co}$O950) before (blue trace) and after CTA (green trace). Resonances associated with the conjugated CTA include the methylene pair (2.17-2.78 ppm) and ester resonances (~4.26 ppm).

and intracellular responsive segments.[15-18] For example, wayakanon et al. prepared polymersomes composed of poly [2-(methacryloyloxy) ethyl phosphorylcholine] (PMPC) and poly[2-(diisopropylamino) ethyl methacrylate] (PDPA) block co-polymers PMPC-PDPA to deliver antibiotics in an attempt to kill intracellular P. gingivalis within monolayers of keratinocytes and organotypic oral mucosal models.[4] While susceptible to antibiotics, P. gingivalis is capable of evading the toxic effects of these agents by residing within gingival keratinocytes. Treatment with the polymersome-encapsulated metronidazole or doxycycline significantly reduced the number of intracellular P. gingivalis in both monolayer and organotypic cultures compared to free antibiotic. In another study Robertson et al. employed PMPC-PDPA to prepare tubular polymersomes and demonstrated successful intracellular delivery of encapsulated bovine serum albumin.[5] Polymersomes have also been employed to prepare stable nanoreactors containing enzymes capable of producing antibiotics at the site of infection.[6] In these studies an amphiiphilic triblock copolymer composed of poly(2-methyloxazoline)-block-poly(dimethylsiloxane)-block-poly(2-methyloxazoline was used to encapsulate the enzyme penicillin acylase. This system protected the enzyme from degradation and showed antibacterial activity under physiological conditions for up to seven days. Brinkhuis and coworkers have investigated the size-dependent pharmacokinetic properties of polymersomes using ^{111}In-labeled polybutadiene-block-poly(ethylene glycol). In these studies the authors found that polymersomes with diameters around 90 nm showed extended circulation times, with greater than 30 % injected dose remaining at 24 h, while polymersomes with sizes greater than 120 nm had largely been cleared from circulation at 4h. Recent advances in controlled radical polymerization (CRP) methodologies have the potential to revolutionize the development of sophisticated multifunctional drug delivery systems.[7-9] Reversible addition-fragmentation chain transfer (RAFT) polymerization in particular has allowed previously unattainable polymeric architectures to be prepared under industrially feasible conditions. A variety of advanced polymeric architectures have been prepared by RAFT polymerization methodology including stars, brushes, polymeric dendrimers, and bottlebrushes.[10, 11-22, 23-25] Herein we detail the development of pH-responsive endosomalytic brushes capable of spontaneously self-assembling into polymersomes to facilitate the intracellular delivery of antibacterial agents.

Results and discussion

RAFT copolymerization of O950 and HEMA and CTA grafting studies. The desired polymeric brushes were prepared by first establishing conditions suitable for the preparation of hydroxyl-functional scaffolds to which the carboxylic functional RAFT agents could then be grafted. These polymers were prepared by copolymerizing HEMA and O950 in dixoane at 70 °C as shown in Scheme 1. Based on our previous studies with O950, CTP and ABCVA were employed as the RAFT agent and initiator respectively at an initial monomer concentration of 20 wt%.[27] As can be seen from Fig. 1 (a-c) these polymerization conditions yield materials with narrow molecular weight distributions over a wide range of copolymer compositions at a fixed initial monomer to CTA ratio

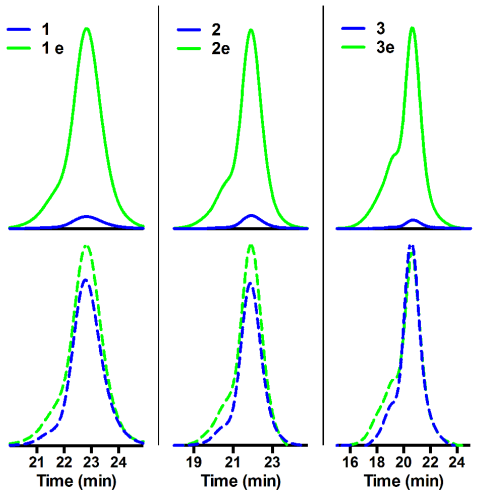

Fig. 2 GPC chromatograms showing conjugation of ECT to polymeric scaffolds with different molecular weights. Poly(HEMA$_{co}$O950) before (blue traces) and after CTA conjugation (green traces) was analyzed via GPC at a constant injection volume of 0.5 mg/mL. (top) Overlay of the UV response at 310 nm where thiocarbonyl thio groups show strong absorbance. (bottom) Overlay of the RI response, which is proportional to the injected mass. Molecular weight (Da), Đ, and number of ECT functional groups per polymer are as follows: (1) 10 500/1.07/1 (1e, graft), 15 700 /1.09/9 (2) 22 500 /1.09/1 (2e, graft) 34 300 /1.19/28.5, and (3) 40 600 /1.15/1 (3e, graft) 68 000/1.19/36. Absolute molecular weights and Đ values where determined via SEC in DMF eluent. The extinction coefficient of ECT in DMF at 310 nm (9422 L mol^{-1} cm^{-1}) was used to determine the concentration of polymer conjugated RAFT agent. The number of ECT functional groups per polymer was then determined by comparing these values to the respective absolute molecular weights determined by SEC.

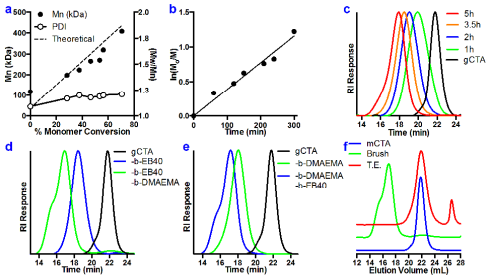

Fig. 3 Kinetic data for the RAFT polymerization of DMAEMA from polymeric graft chain transfer agents (gCTA) containing an average of 34 CTAs/chain at 90 °C in DMSO with V40 as the initiator. The initial monomer ($[M]_o$) to total polymer grafted CTAs ($[gCTA]_o$) to initiator ($[I]_o$) ratio was 100:1:0.02 respectively at an initial monomer concentration of 30 wt. %. (a) M_n versus conversion (b) pseudo first order rate plot. (C) Evolution of the molecular weight distributions with versus time. (d) Molecular weight distributions for the RAFT block copolymerization of DEAEMA and BMA (60:40 molar feed ratio) and DMAEMA from the gCTA in dioxane. (d) poly(EB40-b-DMAEMA)-brush (e) poly(DMAEMA-b-EB40) brush. (f) DMAP catalyzed transesterification of a polymeric brush (green) in methanol releasing scaffold and arm fragments. The disappearance of the brush peek (green) is observed with the appearance of two peeks (red traces) at 22.0 and 26.7 mL. These distributions yield molecular weights of 27 000 and 3300 Da respectively, which are consistent with the anticipated values for the methyl esterified cleaved arm product and the scaffold respectively. The substantial reduction in the scaffold molecular weight is also consistent with transesterificaiton of the O950 ethylene oxide side chains with methanol to yield methyl esters.

($[M]_o/[CTA]_o$) of 50. Experimentally determined molecular weights for these copolymers are in good agreement with theoretically determined values (See supporting information Table 1) and range between 16 000 Da for the 25:75 molar composition of O950/HEMA and 28 000 Da for 75:25 composition with Đ values of 1.07 and 1.18 respectively. Copolymerizations targeting a range of $[M]_o/[CTA]_o$ ratios were also conducted in order to determine the feasibility of preparing polymeric scaffolds with different molecular weights. As can be seen from Fig. 1d, copolymerizations are well controlled at target degree of polymerizations (DP) between 13 and 100 with narrow molecular weight distributions that are symmetric and unimodal. These results as well as the copolymer composition data (determined by ^{1}H NMR) confirm the feasibility of preparing hydroxyl functional scaffolds with variable functional group density and distributions by RAFT. The distribution of the large oligoethylene oxide O950 residues and hydroxyl functional HEMA groups throughout the polymer backbone was evaluated by determining reactivity ratios for the comonomers (r_{O950}, r_{HEMA}) using the inverted Fineman-Ross method.[28] This treatment of the data (Fig. 1e) results in a linear plot for series of copolymerizations of O950 and HEMA over a wide range of molar feed composition yielding reactivity ratios of 0.290 and 1.37 for O950 and HEMA respectively. These values suggest that the addition of HEMA to both growing chains species is favored, which under the RAFT conditions employed, would be expected to yield gradient copolymers that are rich in HEMA at low to moderate comonomer conversions. Copolymer compositions for copolymerizations of O950 and HEMA at molar feed ratios of 25:75, 50:50, and 75:25 are shown in supporting information Table 1. Successful ECT grafting was confirmed via ^{1}H NMR spectroscopy as shown in Fig. 1f. Shown here is a ^{1}H NMR spectrums in $CDCl_3$ for the poly(O950$_{co}$HEMA) macroCTA before (blue trace) and after CTA grafting (green trace). The pregraft sample shows resonances associated with the O950 residues such as the intense O950 ethylene oxide resonance (3.63 ppm) as well as the terminal methoxy resonance at (3.38 ppm) which combined with the overlapping HEMA and O950 ester resonances at 3.87 - 4.24 ppm allow for direct determination of the copolymer composition. Following CTA grafting several additional resonances are visible (Fig. 1f green trace) including new ester resonances at 4.26 ppm as well as resonances at 2.17-2.78, 1.95, and 1.37 ppm that are consistent with the expected shifts for ECT grafted methylene pair as well as the methyl groups present on the CTA R and Z groups respectively.

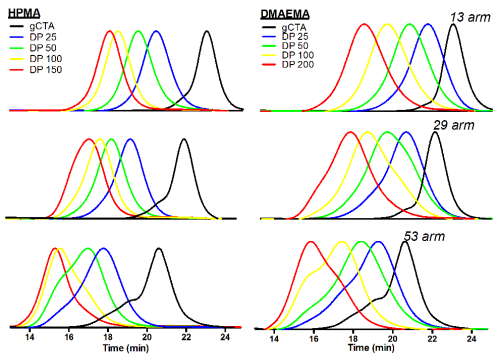

Fig. 4 Normalized refractive index response versus time for the RAFT polymerization of HPMA and DMAEMA from graft chain transfer agents containing 13, 29, and 53 thiocarbonyl thio groups per polymer. Polymerizations of HPMA were conducted in molecular grade water at an initial monomer concentration of 15 wt. % for 4 hours at 70 °C with ABCVA as the initiator. Target degrees of polymerization evaluated were 25, 50, 100, and 150 with an initial thiocarbonyl thio group to initiator ratio of 0.05. Polymerizations of DMAEMA were conducted in DMSO at an initial monomer concentration of 20 wt. % for 4 hours at 70 °C with ABCVA as the initiator. Target degrees of polymerization evaluated were 25, 50, 100, and 200 with an initial thiocarbonyl thio group to initiator ratio of 0.01.

CTA grafting studies were conducted with a copolymer with a molecular weight of 20 500 Da and a comonomer composition consisting of 38 mol % O950 and 62 mol % HEMA (50:50 O950/HEMA in the feed). This composition yields a high hydroxyl group density relative to the number of repeat units while the overall copolymer consists of only 18 % HEMA by mass. Additionally, this composition maximizes the solubility of resultant graft copolymers in a range of solvents and provides favorable bulk physical properties similar to poly(O950). Grafting of the trithiocarbonate based RAFT agent, ECT, to the polymeric scaffolds was achieved using DCC and DMAP in methylene chloride with a two molar excess of these reagents relative to HEMA hydroxyl residues. Trithiocarbonates-based RAFT agents containing a cyanovaleric acid R-group were selected because these agents have been shown to provide excellent control for the polymerization of a variety of monomer families including methacrylates, acrylamides, and methacrylamido monomers at higher initial $[CTA]_o/[I]_o$ ratios relative to dithiobenzoate-based CTAs.[24,29-31] These low radical conditions are particularly important for preparing well-defined brushes where there are numerous potential locations for chain breaking termination reactions to occur. Fig. 2 shows the molecular weight distribution for poly($O950_{co}$HEMA) copolymers (DP 12.5, 25, and 50) before and after CTA grafting reactions. As can be seen from Fig. 2, molecular weight distributions for both traces (injected at identical concentrations) show similar relative peek sizes as determined by the refractive index detector. In contrast the UV absorbance traces at 310 nm, where the polymer backbone shows negligible absorbance but thiocarbonyl thio groups show strong absorbance, is significantly enhanced for the copolymer following CTA grafting. This result suggests that a large number of trithiocarbonate groups were successfully grafted to the polymer backbone. Also apparent from Fig. 2a and b is the lack of any significant asymmetry in the molecular weight distributions following CTA grafting. This result suggests that chain coupling reactions are not observed under these grafting conditions. The resultant CTA grafts are linked via ester bonds to the R group yielding a polymeric graft chain transfer agent (gCTA) that is expected to polymerize from the central scaffold to from brush-like materials. This architecture is advantageous for materials designed for use in vivo as it provides a mechanism by which high molecular weight single polymer nanoparticles (SPNs) can be degraded to molecular weights suitable for clearance by hydrolysis and potentially via esterase activity.

Kinetic evaluation of the polymerization of DMAEMA from a poly($HEMA_{co}O950$) gCTA. Polymerization kinetics were evaluated from the 34-arm gCTA using the methacrylate monomer dimethylaminoethyl methacrylate (DMAEMA). This monomer has been employed by our group and others to condense nucleic acids and as part of pH-responsive endosomal releasing systems.[32-34] The RAFT polymerization of DMAEMA from the 34-arm gCTA was conducted at 90 °C in DMSO using ABCC as the initiator. The initial monomer to polymer bound CTAs ($[M]_o/[gCTA]_o$) was 100. In order to minimize chain-chain coupling reactions the radical concentration was kept low by employing a relatively high initial chain transfer to initiator ratio ($[gCTA]_o/[I]_o$) of 50 to 1. The results of these studies are shown in Fig. 3a-c. Under these conditions the M_n versus conversion plot for the copolymerization of DMAEMA remains linear up to relatively high monomer conversion (70%) with low Đ and good agreement with the theoretical molecular weights (Fig. 3a). Analysis of the resultant copolymers show that an overall monomer conversion of 70.5 % is reached at 5 h with a molecular weight and Đ of 409 000 Da and 1.21, respectively. Given the close agreement between the theoretical and experimental molecular weights under these conditions, it is likely that brush-brush coupling and degradative chain transfer reactions are not occurring to a significant extent. Similarly, the pseudo first order rate plot versus time (Fig. 3b) is also linear suggesting that termination reactions remain low throughout the course of the polymerization. Moreover, analysis of the molecular weight distributions (MWDs) (Fig. 3c) shows that the peaks remain unimodal and symmetric throughout the course of the polymerization and shift to lower elution volumes with time. The lack of significant low molecular weight tailing in the MWDs coupled with the absence of high molecular weight shouldering suggest that the RAFT polymerization of DMAEMA from the 34 gCTA is indeed living under these conditions. The conditions outlined above were subsequently also employed to prepare brushes with arms consisting of diblock copolymers. In these studies the 34-arm gCTA was first employed to prepare a polymeric

Table 1. Theoretical and experimentally determined molecular weight values and Đ for the RAFT polymerization of HPMA and DMAEMA target a range of target DPs from graft chain transfer agents containing 13, 29, and 53 thiocarbonyl thio groups per polymer.

Polymer	Monomer	Target DP d	Arms	Conversionb	Mn Theory d	Mn Exp a	Đ a
1	**HPMA**	25	13	81	53,267	53,480	1.16
2	**HPMA**	50	13	77	87,300	86,690	1.16
3	**HPMA**	100	13	71	148,800	158,300	1.13
4	**HPMA**	150	13	62	188,764	199,300	1.14
5	**HPMA**	25	29	86	123,453	112,200	1.19
6	**HPMA**	50	29	72	184,523	184,000	1.2
7	**HPMA**	100	29	62	291,618	276,200	1.17
8	**HPMA**	150	29	53	367,443	371,100	1.3
9	**HPMA**	25	53	85	228,624	231,500	1.39
10	**HPMA**	50	53	76	354,769	399,800	1.36
11	**HPMA**	100	53	61	532,520	689,500	1.35
12	**HPMA**	150	53	60	745,277	948,900	1.37
13	**DMAEMA**	25	13	83	57,882	69,100	1.25
14	**DMAEMA**	50	13	69	86,136	127,000	1.27
15	**DMAEMA**	100	13	47	111,377	158,600	1.26
16	**DMAEMA**	200	13	40	179,228	251,900	1.25
17	**DMAEMA**	25	29	90	136,310	138,600	1.32
18	**DMAEMA**	50	29	63	178,823	170,100	1.45
19	**DMAEMA**	100	29	41	222,590	269,400	1.41
20	**DMAEMA**	200	29	25	262,255	451,800	1.31
21	**DMAEMA**	25	53	88	251,307	289,800	1.49
22	**DMAEMA**	50	53	62	327,546	381,300	1.55
23	**DMAEMA**	100	53	60	570,427	760,400	1.42
24	**DMAEMA**	200	53	55	989,534	1,187,500	1.36

a As determined by size exclusion chromatography using Tosoh SEC TSK-GEL α-3000 and α-4000 columns (Tosoh Bioscience, Montgomeryville, PA) connected in series to an Agilent 1200 Series Liquid Chromatography System (Santa Clara, CA) and Wyatt Technology miniDAWN TREOS, 3 angle MALS light scattering instrument and Optilab TrEX, refractive index detector (Santa Barbara, CA). HPLC-grade DMF containing 0.1 wt.% LiBr at 60 °C was used as the mobile phase at a flow rate of 1 mL/min.

b As determined by ^{1}H NMR in $CDCl_3$ by comparison of the vinyl resonances present (4.86/5.39 for DMAEMA and 5.36/5.60 for HPMA) on the monomer to either the combined ester resonances at 3.26-3.60 ppm for DMAEMA) or the C**H**(OH)resonance at 3.85 ppm for HPMA.

c As determined by the equation M_n theory = $[M]_o * C_M * FW_M / [ECT]_o$ where $[ECT]_o$ is the total concentration of ECT groups linked to the gCTA (including the chain end) as determined by UV spectroscopy in DMF using an extinction coefficient for ECT of 9400 L/mol.

brush with either DMAEMA or a combination of DEAEMA (E) and BMA (B) in a 60:40 molar ratio. The latter combination has been shown to exhibit potent pH-sensitive red blood cell lysis.[35] The pH value at which this transition from inactive to membrane destabilizing occurs is controllable by simple manipulation of the stoichiometric ratio of the two comonomers. Following isolation of the two polymeric brushes a second polymeric segment was added to yield diblock copolymer brushes with architectures illustrated in Supporting Information Scheme 1. A linear diblock copolymer was also prepared in order to provide a control for subsequent solution studies. The results of these polymerizations are highlighted in Fig. 3d, e where a clear shift of the molecular weight distribution to lower elution volumes is observed for the both DMAEMA and the EB40 polymerizations. Apparent from these traces is the lack of significant tailing or any appreciable low molecular weight species. The resultant poly(DMAEMA) (Mn = 227 600 Da; Đ = 1.28) and poly(EB40) (Mn = 282 700 Da; Đ = 1.20) brushes were then employed as macro gCTAs to prepare diblock copolymer brushes with the opposite monomer compositions (ie. DMAEMA block EB40 and EB40 block DMAEMA). The final poly[(DMAEMA)-b-(EB40)] and poly[(Eb40)-b-(DMAEMA)] brushes had molecular weights and Đ of 670 000/1.25 and 719 000/1.27 respectively. After subtraction of the parent gCTA molecular weight from the polymeric brushes (as determined by GPC) and division by the average number ECT grafts(determined via UV spectroscopy) an average molecular weight per arm of 5600 /13 000 and 7200/12 800 was determined for the DMAEME$_b$EB40 and EB40$_b$DMAEMA mono-/di-block copolymer brushes respectively. While the latter numbers are somewhat inflated due to the presence of some increased chain termination. The aqueous solution properties of these diblock copolymer brushes as well as the linear control including pH-dependent dynamic light scattering and red blood cell hemolysis as well as static light scattering and fluorescent CMC measurements are shown in Supporting information.

In order to further confirm the formation of the predicted polymeric brushes polymer degradation studies were conducted (Fig. 3f). In these studies the brushes were degraded into their constituent components by conducting DMAP catalyzed transesterification reactions in refluxing methanol. These synthetic conditions were employed in order to yield soluble materials that could be easily evaluated via GPC without producing insoluble or column interactive (in DMF) ionic species. The product of these reactions liberate the covalently

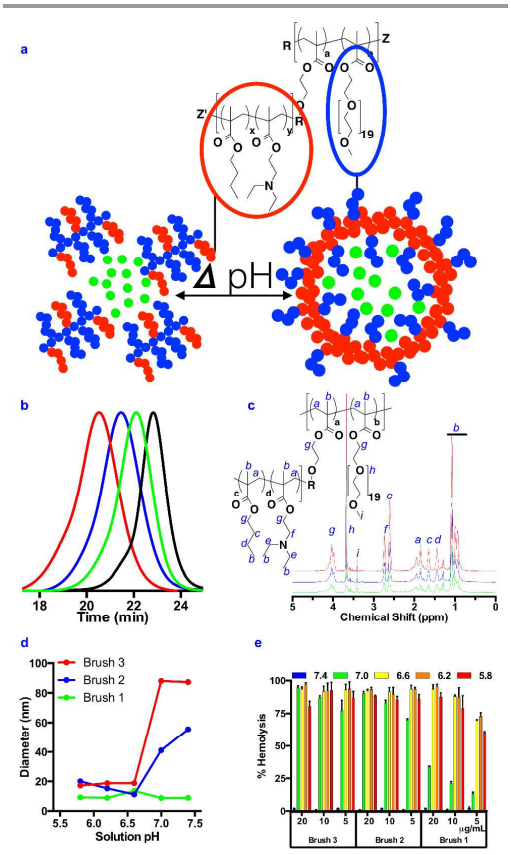

Fig. 5 (a) Schematic representation showing the pH-dependent self-assembly of polymeric brushes into polymersomes. Polyethylene oxide segments are introduced into the polymer backbone via the copolymerization of HEMA with O950 stabilizing the short polymeric segments poly(DEAEMA$_{co}$BMA) that are introduced via subsequent copolymerization of the corresponding comonomers in the presence of gCTAs 1-3. (b) Molecular weight distributions for the gCTA and corresponding EB40 brushes. (c) ^{1}H NMR in $CDCl_3$ confirming copolymer composition. pH-dependent (d) Dynamic light scattering (e) red blood cell hemolysis for the three EB40 brushes with longer EB40 segments showing larger sizes at pH 7.0 and 7.4 and enhanced concentration dependent red blood cell lysis.

attached polymeric grafts, which are attached to the cyanovaleric acid R group via ester bonds, from the scaffold resulting in methyl esters. Additionally the polymeric scaffold could also be expected to reduce in molecular weight as a result of methyl ester formation. This reaction would substantially reduce the molecular weight of scaffold by replacing long O950 ethylene oxide segments with methyl esters. As can be seen in Fig. 3f, the poly(HEMA$_{co}$O950) macroCTA (blue trace) elutes at around 29.6 mL with the resultant poly(EB$_b$DMAEMA) brush (green trace) shifted to around 17.0 mL. Following reflux in methanol containing DMAP for 96 hours a disappearance of the brush peek is observed with the appearance of two peeks (red traces) at 22.0 and 26.7 mL. These distributions yield molecular weights of 27 000 and 3300 Da respectively, which are consistent with the anticipated values for the methyl esterified cleaved arm product and the scaffold respectively. The substantial reduction in the scaffold molecular weight is also consistent with transesterificaiton of the O950 ethylene oxide side chains with methanol to yield methyl esters. Based on a DP of 53 for the macroCTA the corresponding poly(methyl methacrylate) would be expected to have a molecular weight of ~5200 Da which is in reasonable agreement with the experimental values given the low light scattering signal observed.

Synthesis of N-(2-Hydroxypropyl)methacrylamide (HPMA) and DMAEMA with variable arm and target DPs. The ability to prepare polymeric brushes with different degrees of polymerization was also evaluated. In these studies, the gCTAs detailed in Fig. 2 were used to prepare a series of brushes with different target degrees of polymerization for gCTAs with 13, 29, and 53 arms. Both HPMA and DMAEMA were evaluated using polymerization conditions developed specifically for the methacrylamido and methacrylate monomers. Shown in Fig. 4 and detailed in Table 1 are the results of these polymerizations targeting DPs of 25, 50, 100, and 150 for HPMA and 25, 50, 100, and 200 for DMAEMA. In all cases a clear shift in the molecular weight chromatograms (refractive index traces shown) are observed. Exceptionally good polymerization control is observed for the synthesis of both HPMA and DMAEMA brushes with 13 and 29 arms. These polymerizations yield materials with narrow symmetric molecular weight distributions that cleanly shift to lower elution volumes. Moreover the resultant chromatograms show only small amounts of brush-brush coupling as evidenced by the lack of significant high molecular weight shouldering. Also apparent is the lack of peeks at longer elusions volumes, which confirms the absence of observable low molecular weight unimeric polymer species. Under these conditions HPMA brushes with molecular weights and Đ values of 158 300 Da/1.13 and 276 200 Da/1.17 are observed for the 13 and 29 arm gCTAs targeting a DP of 100 while DMAEMA brushes, also targeting a DP of 100, show values of 158 600 Da/1.26 and 269 400 Da/1.41 respectively. Relatively good control is also observed for the 53 arm brushes although the appearance of high molecular weight shoulder is apparent especially at the higher target DPs. Similar to the lower arm gCTAs these materials all cleanly shift to lower elution volumes without showing the presence of appreciable low molecular weight populations. It should be noted that brushes prepared under these conditions with HEMA yielded materials with broad molecular weight distributions presumably from transesterification at the elevated reaction temperatures. Similarly polymerizations of PEGMA monomers (O300 and O950) from both dithiobenzoate- and trithiocarbonate-based gCTAs yield disperse materials with high molecular weights (not shown). These results could be a result of low addition

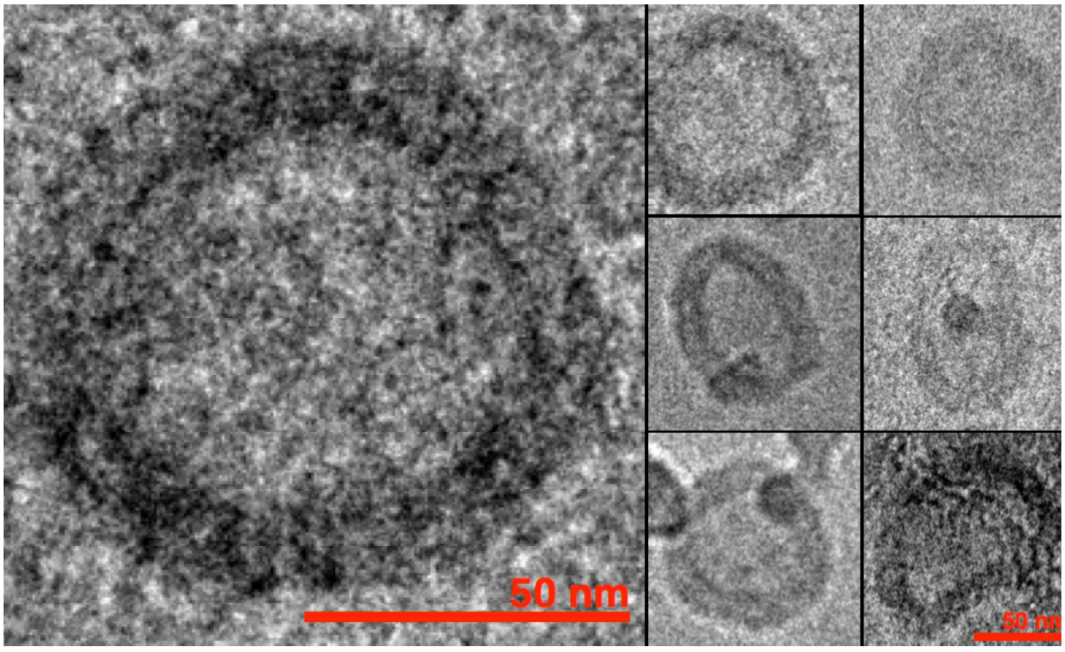

Fig. 6 CryoTEM image of polymersomes derrived from pH-responsive brush copolymer 3. The morphology of polymersomes was visualized by cryoTEM using the freeze-plunging method. During the sample examination, the temperature of cryoholder was maintained at -179°C to prevent sublimation of vitreous water.

and/or high fragmentation rates to the growing polymeric brushes by the stericly bulky PEGMA monomers.

Synthesis of pH-responsive polymersomes. Shown in Fig. 5a is a schematic representation of pH-responsive polymeric brushes self-assembling into polymersomes. In this design O950 residues present in the polymeric scaffold stabilized the nanostructures in aqueous solution while short segments of DEAEMA and BMA (60:40 molar feed percent) (EB40) serve as the endosomalytic trigger. In order to investigate the structure-dependent morphologies of this design a series of brushes with different molecular weight EB40 polymeric arm lengths were synthesized. The resultant polymeric brushes have narrow and symmetric molecular weight distributions Fig. 5b) that cleanly move to lower elution volumes and ^{1}H NMR confirms that all three copolymers have monomer compositions that are similar to the feed (Fig. 5c). At low pH-values the polymeric brushes are molecularly soluble but an increase in solution pH triggers self-assembly. This pH-dependent behavior can be seen in Fig. 5d by following the hydrodynamic diameter, via dynamic light scattering (DLS), as a function of pH for the three brushes. At pH values of 5.8, 6.2, and 6.6 all three brushes show diameters that are consistent with molecularly dissolve materials. Above this pH values a transition occurs causing a significant increase in diameter for brushes 2 and 3 while brush 1, which has the shortest EB40 segment remains unimeric over the entire pH range. For example, brush 3, which has a molecular weight of 105 000 Da with an average of ~13 arms and a molecular weight per EB40 arm of 6900 Da, shows hydrodynamic diameters of 17.2 nm and 87.4 nm at pH 5.8 and 7.4 respectively. Polymer 2, which has slightly shorter EB40 arms of approximately 4100 Da, also shows a large increase in diameter at these pH values from 20 to 55 nm respectively while polymer 1 (2600 Da /EB40 arm) remains small at around 9 nm over the entire pH range tested. All three brushes show potent pH-dependent red blood cell lysis with negligible levels of hemolysis at pH 7.4 but increasing levels of red blood cell lysis below this value (Fig. 5e). We have shown previously that the precise pH value at which copolymers of DEAEMA and BMA transition from inert to membrane disruptive can be adjusted simply by changing the feed ratio of these monomers with higher BMA content leading to materials that transition at lower pH values.[35] The morphology of brush 3 was further investigated via cryoTEM as shown in Fig. 6. From Fig. 6 the circular morphology of the self-assembled structures is clearly visible with a strong contrast between the pH-responsive polymer membrane and the aqueous interior. CryoTEM measurements suggest these structures are on the order of 90 nm which is in good agreement with values determined via DLS. The ability of the polymersomes to encapsulate the hydrophilic antibiotic drug ceftazidime was confirmed via HPLC. In these studies drug loading was determined to be mg ceftazidime per g polymer.

Formatted: Font: Bold

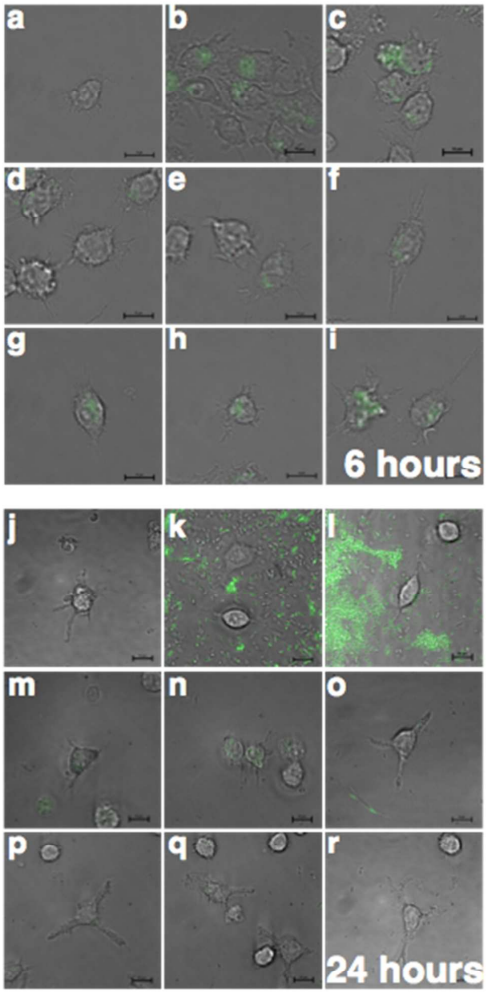

Fig. 7 Fluorescence microscopy of RAW 264.7 cells incubated with B. thailandensis (AH183) containing the pMLS7-eGFP plasmid encoding genes for both green fluorescence protein and trimethoprim resistance. Well were infected for 1 hr, then washed and incubated with 0.25 mg/mL kanamycin for 1 hour to kill extracellular bacteria. Cells incubated for 6 hours with (a) Untreated cells, (b,c) no antibiotic, (d,e) polymersome-encapsulated ceftazidine 0.05 mg/mL, (f) 0.10 mg/mL, (g,h) free ceftazidine 0.05 mg/mL, (i) 0.10 mg/mL. Cells incubated for 24 hours with (j) Untreated cells, (k,l) no antibiotic, (m,n) polymersome-encapsulated ceftazidine 0.05 mg/mL, (o) 0.10 mg/mL, (p,q) free ceftazidine 0.05 mg/mL, (r) 0.10 mg/mL.

the polymersomes almost immediately. These studies (Supporting information Fig. 2) support the dynamic assembly-disassembly of the polymersomes upon internalization into acidic endosomal/lysosomal compartments and provide a mechanism by which intracellular bacteria, which are difficult

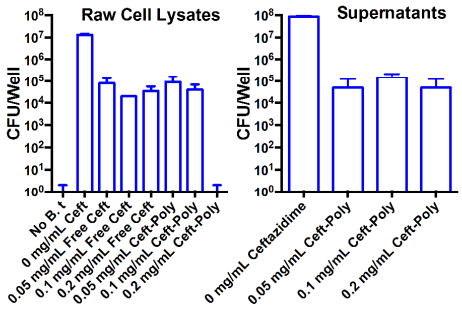

Fig. 8 a, b. Coculture of RAW 264.7 cells with B. thailandensis demonstrating the ability of the polymersome encapsulated ceftazidime to treat both intracellular and extracellular bacteria.

to access with many traditional antibiotics, can potentially be treated.

Intracellular antibacterial activity

Shown in Fig 7 are fluorescence microscopy images for RAW 264.7 cells incubated with incubated with B. thailandensis (AH183) containing the pMLS7-eGFP plasmid encoding genes for both green fluorescence protein and trimethoprim resistance. Well were infected for 1 hr, then washed and incubated with 0.25 mg/mL kanamycin for 1 hour to kill extracellular bacteria. Untreated cells (Fig. 7a,j) show negligible green fluorescence while macrophages incubated with bacteria but no antibiotic for 6 h (Fig. b,c) and 24 h (Fig. k,l) show substantial green fluorescence. In these imaes the fluorescent bacteria are primarily observed to be localized within intracellular compartments at the earlier time point while at 24 hours most of the RAW 264.7 cells have lysed releasing bacteria into the extracellular space. In contrast cells incubated with the polymersome encapsulated ceftazidime show low levels of green fluorescent bacteria at both 6 (Fig. d-f) and 24 (Fig. m-o) hours. The low level of extracellular bacteria even at 24 hours suggests that the polymersomes are able to effectively release the encapsulated antibiotic in a pH-dependent fashion while localized within intracellular compartments Similar results are observed for the unencapsulated ceftazidime at both time points (Fig. g-l, p-r;). Plotted in Fig. 8a, b are the results of a coculture bacterial challenge assay with B. thailandensis and RAW 264.7 cells. A plot of RAW cell lysates show that cells treated with bacteria but no antibiotics have very high levels of intracellular and extracellular bacteria. These values, which are on the order of 1.3 x 10^7 colony forming units per well (CFU/Well), are substantially reduced to around 35 000 CFU/Well for the cell lysates with the addition of 0.2 mg/mL free ceftazidine. This dose, which is above the minimum inhibitory concentration (MIC) for planktonic cultures of B. thailandensis, highlights the differences between the intracellular and extracellular effectiveness of ceftazidime. Pathogens such as *Francisella tularensis and Burkholderia sp.*

have evolved the ability to reside and multiply within lung macrophages, where they are protected from an adaptive immune response and antibiotics. In contrast the cells treated with ceftazidime loaded into intracellular responsive polymersomes show very high levels of bacteria inhibition in both the RAW cell lysates as well as in the supernatants. Cells treated with 0.05 and 0.1 mg/mL show intracellular bacteria levels comparable with the highest does of ceftazidime, while at a dose of 0.2 mg/mL the intracellular bacteria load is reduced to undetectable levels. A small level of bacteria is observed in the extracellular fractions (e.g. 50 000 CFU/Well) at 0.2 mg/mL however this level is 1700 times lower than the untreated cells. The low intrinsic toxicity of the polymeric brush used in these studies was confirmed by an MTS assay where greater than 93 % cell viability was observed even at polymer concentrations as high as 2.0 mg/mL (See supporting information).
These results taken together suggest that the ceftazidime is being retained to a significant degree within the polymersomes until endosomal acidification causes spontaneous disassembly resulting in burst drug release as well as endosomal disruption.

Conclusions

RAFT copolymerizations of HEMA and O950 in the presence of the dithiobenzoate-based RAFT agent CTP yield narrow and symmetric molecular weight distributions with controllable compositions and molecular weights. Reactivity ratio measurements suggest that the addition of HEMA to the growing chain ends is favored resulting in copolymers with a gradient structure. The resultant hydroxyl functional copolymers can be employed as scaffolds to which RAFT CTAs can be grafted using DCC/DMAP chemistry. These resultant gCTAs retain the narrow and symmetric molecular weight distributions of the parent scaffolds while showing substantial increases in UV absorbance at 310 nm, which is attributed to the addition of multiple CTAs. At an initial $[CTA]_o/[I]_o$ ratio of 50 polymerizations of DMAEMA pseudo first order rate and M_n vs. conversion plots are linear 70 % monomer conversion. Polymerizations of DMAEMA targeting $[M]_o/[CTA]_o$ ratio between 25 and 200 yield narrow molecular weight distributions with molecular weights that are in good agreement with theoretical values for 34 arm brushes. Transesterifcation of the brushes with DMAP in methanol yields degradation products that are consistent with calculated molecular weights for the polymeric methyl esters of the arms and scaffold. A combination of DLS and cryoTEM confirmed the formation of pH-responsive polymersomes from polymeric brushes with short EB40 segments. Cells treated with ceftazidime loaded into intracellular responsive polymersomes show very high levels of bacteria inhibition in both the RAW 264.7 cell lysates as well as in the supernatants. Cells treated with 0.05 and 0.1 mg/mL show intracellular bacteria levels comparable with the highest does of ceftazidime, while at a dose of 0.2 mg/mL the intracellular bacteria load is reduced to undetectable levels. These results demonstrate the potential of endosomal-responsive polymersomes as potent antibiotic drug carriers capable of reaching persistent intracellular bacteria.

Experimental

Materials Chemicals and all materials were supplied by Sigma-Aldrich unless otherwise specified. Diethylaminoethyl methacrylate (DEAEMA), Dimethylaminoethyl methacrylate (DMAEMA), and Hydroxyethyl methacrylate (HEMA) were distilled under reduced pressure. Spectra/Por regenerated cellulose dialysis membranes (6-8 kDa cutoff) were obtained from Fisher Scientific. Butyl methacrylate (BMA) was passed through a short column of basic alumina. 4-Cyano-4-(phenylcarbonothioylthio)pentanoic acid (CTP) was purchased from Sigma-Aldrich. 4-Cyano-4-(ethylsulfanylthiocarbonyl) sulfanylpentanoic acid (ECT) was synthesized as described previously.[26] Sephedex G-25 prepacked PD10 columns were obtained from GE Life Sciences.

Gel permeation chromatography (GPC). Absolute molecular weights and dispersity indices were determined using Tosoh SEC TSK-GEL α-3000 and two α-e4000 columns (Tosoh Bioscience, Montgomeryville, PA) connected in series to an Agilent 1200 Series Liquid Chromatography System (Santa Clara, CA) and Wyatt Technology miniDAWN TREOS, 3 angle MALS light scattering instrument and Optilab TrEX, refractive index detector (Santa Barbara, CA). HPLC-grade DMF containing 0.1 wt.% LiBr at 60 °C was used as the mobile phase at a flow rate of 1 mL/min.

Cryogenic Transmission Electron Microscopy (CryoTEM). The morphology of polymersomes was visualized by cryoTEM. The samples were prepared using the freeze-plunging method. Briefly, a small droplet of polymersome suspension (ca. 6 µl) was placed on a holey carbon film supported on a TEM copper grid (Electron Microscopy Sciences, Hatfield, PA), which was glow-charged in air before use. The excess solution was removed by blotting with a slip of filter paper (Whatman, Pittsburgh, PA) to form a thin liquid film on the grid. The specimen was then rapidly frozen by plunging into liquid ethane and stored in liquid nitrogen until it was transferred to a cryo-holder (Gatan 626) for examination via a Tecnai G2 F20 electron microscope (FEI Co., Hillsboro, OR). The TEM was operated at an acceleration voltage of 200 keV and images were recorded under a low-dose condition at a magnification of 25,000 or 50,000 by a CCD camera system (4k Eagle Camera, FEI). During the sample examination, the temperature of cryoholder was maintained at -179°C to prevent sublimation of vitreous water.

Dynamic Light Scatttering Measurements. Dynamic light scattering studies of the polymeric brushes were conducted using a Malvern Instruments Zetasizer Nano series instrument equipped with a 22 mW He-Ne laser operating at 632.8 nm. Lyophilized polymer was dissolved in ethanol at 50 mg/mL, then diluted 50-fold into the appropriate acetate or phosphate buffer solution to a final ionic strength of 150 mM.

Red Blood Cell Hemolysis Assay. pH responsive membrane destabilizing activity was assayed by titrating polymer stocks

into preparations of human red blood cells (RBCs) and determining membrane-lytic activity by hemoglobin release (determined by measuring absorbance at 540 nm) under five different pH conditions. RBCs were isolated by centrifugation from whole blood collected in vaccutainers containing EDTA. RBCs were washed 3 times in normal saline and brought to a final concentration of 2% RBCs in PBS at a specific pH (5.8, 6.2, 6.6, 7.0, or 7.4). Polymer samples were evaluated at 10, 20, and 40 μg/mL in triplicate at each pH. Samples were incubated at 37 °C for 60 min and centrifuged to remove intact RBCs. Supernatants were transferred to a transparent 96-well plate, and absorbance was determined at 540 nm. Percent hemolysis is expressed as A540 sample/A540 of 1% Triton X-100 treated RBCs (control for 100% lysis).

RAFT copolymerization of hydroxyethyl methacrylate (HEMA) and poly(ethylene glycol) methyl ether methacrylate (FW_{avg} ~ 950 Da) (O950). Poly($HEMA_{co}$O950) was synthesized at 70 °C with CTP and 4,4′-Azobis(4-cyanovaleric acid) ABCVA as the RAFT chain transfer agent (CTA) and radical initiator respectively. Polymerizations were conducted at initial molar ratios of HEMA to O950 of 25:75, 50:50, and 75:25 with total initial monomer to CTA ratios ([M]o/[CTA]o) between 13 and 100 at a total initial monomer concentration of 20 weight % in inhibitor free dioxane. The initial CTA to initiator ratio ($[CTA]_o/[I]_o$) was 10 for all copolymerizations of HEMA and O950. A representative procedure for the synthesis of poly($HEMA_{co}$O950) targeting a degree of polymerization (DP) of 50 with an equimolar feed ratio of O950 and HEMA is as follows. To a 50 mL round bottom flask was added O950 (5.00 g, 5.26 mmol), HEMA (0.685 g, 5.26 mmol), CTP (59 mg, 0.210 mmol), ABCVA (5.9 mg, 0.021 mmol), and 22.7 mL dioxane. The polymerization solution was then sealed with a rubber septum and purged with nitrogen for 60 minutes. After this time, the polymerization solution was transferred to a preheated oil bath at 70 °C and allowed to polymerize for 18 hours. Following polymerization, the total monomer conversion was determined via HPLC by comparison of the UV absorbance peek areas for the polymerization solution relative to samples taken at time 0. The copolymer was isolated by adding 5 mL of the polymerization solution to 45 mL of diethyl ether in 50 ml conical tubes. After vortexing the soluitons were centrifuged at 4200 rpm for 10 minutes. After this time the clear ether solution was decanted and pink polymer oil was diluted 1 to 1 with acetone and reprecipitated into ether as described above (x6). It is important not to cool the ether as this will cause the O950 monomer to precipitate. The final copolymer composition was determined via ^{1}H NMR in $CDCl_3$ by comparison of the total ester resonances (X) between 3.9 and 4.3 ppm (2H HEMA, 2H O950) to the OCH3 PEGMA resonance (Y) at 3.38 ppm using the following relationships: 1H O950 = Y/3 and 1H HEMA = (X-2Y)/2.

Determination of copolymer reactivity ratios for HEMA and O950. A series of copolymers of HEMA and O950 with different comonomer feed ratios were prepared as described above except that the polymerization times were reduced to 45 minutes to limit monomer conversion. The resultant polymers were isolated by repeated precipitation from acetone into diethyl ether followed by further dialysis against acetone and then against water in Spectra/Por dialysis tubing (1 kDa cutoff). The final polymers were then lyophilized and redissolved in $CDCl_3$ for ^{1}H NMR analysis.

ECT grafting to Poly($HEMA_{co}$O950). CTA grafting reactions were conducted in methylene chloride at 10 wt % copolymer using dicyclohexyl carbodiimide (DCC) and dimethylaminopyridine (DMAP). The initial molar ratio of ECT to polymeric hydroxyl groups was 2 with equimolar quantities of DCC and DMAP relative to ECT. The polymer, DMAP, and ECT were first dissolved in methylene chloride and then allowed to cool to -20 °C after which the DCC was dissolved. The solution was then allowed to react for 8 hours at 5 °C after which time it was filtered to remove the DCU and then isolated by adding 5 mL of the reaction solution to 45 mL of diethyl ether in 50 ml conical tubes. After vortexing the solutions were centrifuged at 4200 rpm for 10 minutes. After this time the clear ether solution was decanted and the yellow/orange polymer oil was diluted 1 to 1 with acetone and reprecipitated into ether as described above (x8). The final graft copolymer was then dried under high vacuum for overnight. A representative procedure is as follows: To a 50 mL round bottom flask was add poly($HEMA_{co}$O950) (2.5 g, 3.5 mmol OH), DMAP (0.857 g, 7.0 mmol), ECT (1.85 g, 7.0 mmol) and dichloromethane (33 mL). After the reagents had completely dissolved the round bottom flask was sealed with a glass stopper and placed in the freezer for 1 hour. After this time DCC (1.45 g, 7.0 mmol) was added and vortexed until it was completely dissolved after which time the solution was placed in the refrigerator and allowed to react for 8 hours. The graft chain transfer agent was then isolated as described above and then characterized by ^{1}H NMR, GPC, and UV-Vis spectroscopy. The total number of ECT grafts per polymer was determined based on the extinction coefficient of ECT and the absolute molecular weight of the gCTA as determined by GPC.

Kinetic evaluation of the RAFT polymerization of DMAEMA. The RAFT polymerization of DMAEMA from a 34 arm gCTA was conducted with 1,1′-azobis(cyclohexanecarbonitrile) (ABCC) as the initiator at 90 °C at an initial monomer concentration of 30 weight %. Subsequent block copolymerizations were diluted according to the following equation. Msolvent = (total mass monomer-f*total mass monomer)/f +(M polymer/2) where f is the desired mass fraction of monomer relative to solvent. The initial monomer ($[M]_o$) to total polymer grafted CTAs ($[gCTA]_o$) to initiator ($[I]_o$) ratio was 100:1:0.02 respectively. Individual polymerization solutions were transferred to a septa-sealed vial and purged with nitrogen for 30 minutes. After this time, the polymerization vials were transferred to a preheated oil bath at 90 °C and allowed to polymerize for the prescribed time period. A representative procedure for the synthesis of a 34 arm poly(DMAEMA) brush (Mn 37 500 g/mol, Đ = 1.15) is as follows: To a 25 mL round bottom flask was added DMAEMA (4.61 g, 29.3 mmol), gCTA (0.30 g, 0.293 mmol ECT), DMSO

(10.8 g), and ABCC (1.43 mg, 5.86 µmol). The polymerization solution was then purged with nitrogen for 30 minutes and then transferred to a preheated oil bath at 90 °C and allowed to react for 5 hours. Following polymerization, the polymer was transferred to Spectra/Por regenerated cellulose dialysis tubing (6-8 kDa cutoff) and dialyzed against acetone at 4 °C for three days with an acetone change each day. After this time the polymer was isolated via rotary evaporation followed by drying under high vacuum. The final molecular weight, Đ, and composition of the poly(DMAEMA) brush was 227 600 Da, 1.28. Monomer conversions were determined via ^{1}H NMR spectroscopy by diluting the polymerization solutions in CDCl3 and comparing the DMAEMA vinyl resonances at 4.86 and 5.40 ppm normalized to the combined monomer and polymer ester resonance at between 3.29 and 3.62 ppm. Polymerizations of DMAEMA targeting DPs between 25 and 200 were conducted in DMSO at an initial monomer concentration of 20 wt. % for 4 hours at 70 °C with ABCVA with an initial thiocarbonyl thio group to initiator ratio of 0.01.

Synthesis of HPMA brushes. Polymerizations of HPMA from gCTAs 1-3 were conducted in molecular grade water at an initial monomer concentration of 15 wt. % for 4 hours at 70 °C with ABCVA as the initiator. Target degrees of polymerization evaluated were 25, 50,100, and 200 with an initial thiocarbonyl thio group to initiator ratio of 0.05. A representative procedure for the synthesis of an HPMA brush from gCTA 1 is as follows: To a 5 mL round bottom flask was added HPMA (0.293 g, 2.04 mmol), gCTA 1 (0.100 g, 82 µmol ECT equivalents), and molecular grade water (1.66 mL). After the contents had completely dissolved ABCVA (1.14 mg, 4.09 µmol) was added as 100 µL of a 11.4 mg/mL stock solution in ethanol. The polymerization solution was then septa sealed and purged with nitrogen for 30 minutes. After this time the polymerization was transferred to a preheated water bath at 70 °C and allowed to react for 4 hours.

Co-culture infection assay.

24-well TC-treated plates were seeded with RAW 264.7 murine macrophage cells at a seeding density of 300,000 cells/well in complete growth medium (DMEM+10%FBS, no antibiotic) followed by 16-hr incubation at 37°C, 5% CO_2. *B. thailandensis* (E264) for infection were prepared as follows. 5mL of LB was inoculated with a single colony from an LB-agar plate streaked from glycerol stocks then incubated for 24-hrs at 37°C, 200RPM. The following day, the 24-hr culture was diluted 1:100 in 50mL LB and incubated at 37°C, 200RPM until the culture reached early log-phase (OD=0.2).

RAW 264.7 cells were infected, by replacing cell culture medium with 0.5mL/well complete growth medium containing *B. thailandensis* at a MOI=5 ($1.5x10^6$ CFU/well). Infected RAW 264.7 cells were then incubated at 37°C, 5% CO_2 for 1 hr. Wells were then washed with 0.5mL/well PBS and incubated at 37°C, 5% CO_2 for 1 hr with 0.5mL complete growth medium containing 250ug/mL Kanamycin to kill extracellular bacteria. Wells were washed again with 0.5mL/well PBS then incubated with DMEM containing ceftazidime or ceftazidime loaded polymersomes and incubated for an additional 22 hrs at 37°C, 5% CO_2. The following day, infected RAW 264.7 cells were washed three times with 0.5mL/well PBS and lysed with 0.5 mL PBS w/ 0.1% [v/v] Triton X-100 at room temperature for 10 min. Serial dilutions of lysates or cell culture supernatants were then plated on LB agar plates and incubated for 24 hrs at 37°C before counting CFUs.

~~**Fluorescence Microscopy**~~

~~RAW 264.7 cells were seeded in 8-well cover slip chamber slides (SA=0.7cm^2, No. 1.5 glass) at a concentration of 100,000 cells/well in complete growth media without phenol red or antibiotics and incubated for 16 hrs at 37°C, 5% CO_2. B. thailandensis mutant AH183 which harbors pMLS7-eGFP encoding both the trimethoprim resistance (dhfr) and green fluorescent protein gene, was grown in a similar manner to E264, as indicated above, except with the addition of 50ug/mL trimethoprim to all cultures and plates. Co-culture infection was carried out as indicated above, RAW 264.7 cells were infected at a MOI=5, treated with kanamycin, then treated with ceftazidime or ceftazidime loaded polymersomes. 6 and 24 hrs after infection (4 and 22 hrs after ceftazidime treatment), wells were washed with 0.2mL/well PBS and imaged. Cells were imaged with a Live-Cell Fluorescence Microscope (Nikon Ti-E) equipped with an environmental control chamber. Cells were imaged with a mercury lamp and a 100X objective using brightfield and GFP channels [480/40 nm (EX) and 535/50 nm (EM)].~~

HPLC Analysis.

Samples were analyzed using an Agilent 1260 Infinity HPLC system and a Thermo ODS Hypersil reverse phase column (C18, 250x2.1mm). Samples were loaded onto the column in the aqueous mobile phase (30mM Sodium acetate, pH 4.0) and were eluted with a gradient elution with acetonitrile, 0.1% TFA[v/v] as the organic mobile phase at a flow rate of 0.5mL/min.

Fluorescence microscopy. RAW 264.7 cells were seeded in 8-well cover slip chamber slides at a concentration of 5,000 cells/well. After allowing the cells to adhere for 18 hours, media was replaced with media containing ceftazidime loaded polymeric micelles or appropriate controls. Thirty minutes prior to imaging Hoechst (5 µg/mL) was added to the media and allowed to incubate at 37 °C. Immediately prior to imaging, individual wells were treated with 2 µL of a 10 mg/mL cell mask stock in 200 µL of ice cold PBS. After 3 minutes the PBS was removed and washed three times with ice cold PBS. The chamber slides were placed on a Live-Cell Fluorescence Microscope (Nikon Ti-E) equipped with an environmental control chamber. Cells were imaged with a mercury lamp and a 60X objective using the following filter sets: 350/50 nm (EX) and 460/50 nm (EM) for Hoescht, 480/40 nm (EX) and 535/50 nm (EM) for AF488, and 620/60 nm (EX) and 700/75 nm (EM) for Cell Mask Deep red (Chroma 49000 Series, Rockingham, VT). For each image stack, 24 z-sections with a 0.5 um step size were collected using a 1/8 neutral density filter and 400 millisecond exposure. After image acquisition, image stacks

Formatted: Font: Bold

Formatted: Font: Bold

Formatted: Font: Bold

Formatted: Font: Bold

Formatted: 08 Article Text

were deconvolved using object-based measurement software, Volocity (Perkin Elmer), to remove out-of focus fluorescence for the identification of conjugate containing compartments. To deconvolve image stacks, point spread functions were calculated for the green, blue, and far red channel and applied using 25 iterations to reach a near 100% confidence interval.

pH-induced self-assembly of polymersomes. The polymersomes were prepared by adjusting an acidic solution of brush polymers to neutral pH. In detail, brush polymers (25 mg) were first dissolved in acetate buffer (1 mL, 25 mM, pH 4.5) and mixed with phosphate buffer saline (1.5 mL, 10 mM, pH 7.4) containing 50 mg/mL ceftazidime (TCI America, Portland, OR). To induce the formation of ceftazidime-loaded polymersomes, the pH value of the solution was gradually adjusted to pH 7.4 using a 5 N sodium hydroxide solution. The obtained polymersomes were then purified *via* a PD-10 desalting column (GE Healthcare, Piscataway, NJ) to remove the free ceftazidime. The amount of ceftazidime encapsulated in the prepared polymersomes was quantified by high performance liquid chromatography (HPLC, Agilent 1260 Infinity HPLC system) using a reversed-phase C18 column (25 cm × 2.1 mm × 5 µm, Thermo Scientific). The mobile phase was changed linearly from 100% acetate buffer (20 mM, pH 4.0) to 100 % acetonitrile containing 0.1% trifluoroacetic acid for 20 min at a flow rate of 0.5 mL/min. The injection volume for drug analysis was 20 µL and the UV detection was carried out at 275 nm at room temperature. The amount of encapsulated ceftazidime was 0.4 ± 0.07 mg/mL of polymersome suspension. The drug loading content was 5.08 ± 0.97 wt. %.

Formatted: Font: Bold

Formatted: Font color: Text 1

Acknowledgements

This work was funded by the National Institutes of Health (Grant R01EB002991 and Grant 1R21EB014572- 01A1), the Defense Threat Reduction Agency (DTRA) (HDTRA1-13-1-0047), and the Life Science Discovery Fund (Grant 2496490).

Notes and references

[l] Equally contributing co-first authors.

[a] Molecular Engineering and Sciences Institute, Department of Bioengineering, Box 355061, Seattle, WA, 98195, USA. E-mail: aconv@uw.edu; Fax: +1 (206) 685 8526; Tel: +1 (206) 221 5113

† Electronic Supplementary Information (ESI) available: [details of any supplementary information available should be included here]. See DOI: 10.1039/b000000x/

1. N. J. Beeching, D. A. B. Dance, A. R. O. Miller, and R. C. Spencer, *BMJ*, 2002, **324**, 336–339.
2. B. J. Currie, L. Ward, and A. C. Cheng, *PLoS Negl Trop Dis*, 2010, **4**, e900.
3. D. T. Dennis, T. V. Inglesby, D. A. Henderson, J. G. Bartlett, M. S. Ascher, E. Eitzen, A. D. Fine, A. M. Friedlander, J. Hauer, M. Layton, S. R. Lillibridge, J. E. McDade, M. T. Osterholm, T. O'Toole, G. Parker, T. M. Perl, P. K. Russell, K. Tonat, and F. T. W. G. O. C. Biodefense, *JAMA*, 2001, **285**, 2763–2773.
4. K. Wayakanon, M. H. Thornhill, C. W. I. Douglas, A. L. Lewis, N. J. Warren, A. Pinnock, S. P. Armes, G. Battaglia, and C. Murdoch, *FASEB J.*, 2013, **27**, 4455–4465.
5. J. D. Robertson, G. Yealland, M. Avila-Olias, L. Chierico, O. Bandmann, S. A. Renshaw, and G. Battaglia, *ACS nano*, 2014, **8**, 4650–4661.
6. K. Langowska, C. G. Palivan, and W. Meier, *Chemical Communications*, 2013, **49**, 128–130.
7. G. Moad, E. Rizzardo, and S. H. Thang, *Australian Journal of Chemistry*, 2012, **65**, 985–1076.
8. D. S. H. Chu, J. G. Schellinger, J. Shi, A. J. Convertine, P. S. Stayton, and S. H. Pun, *Acc. Chem. Res.*, 2012, **45**, 1089–1099.
9. P. J. Roth, C. Boyer, A. B. Lowe, and T. P. Davis, *Macromolecular Rapid Communications*, 2011, **32**, 1123–1143.
10. M. H. Stenzel and T. P. Davis, *Journal of Polymer Science Part A: Polymer Chemistry*, 2002, **40**, 4498–4512.
11. M. H. Stenzel Rosenbaum, T. P. Davis, A. G. Fane, and V. Chen, *Angewandte Chemie*, 2001, **113**, 3536–3540.
12. M. Stenzel Rosenbaum, T. P. Davis, V. Chen, and A. G. Fane, *Journal of Polymer Science Part A: Polymer Chemistry*, 2001, **39**, 2777–2783.
13. A. Li, J. Ma, G. Sun, Z. Li, S. Cho, C. Clark, and K. L. Wooley, *Journal of Polymer Science Part A: Polymer Chemistry*, 2012, **50**, 1681–1688.
14. Chun-Yan Hong, A. Ye-Zi You, and C.-Y. Pan, *Chemistry of materials*, 2005, **17**, 2247–2254.
15. Debashish Roy, A. James T Guthrie, and S. Perrier, *Macromolecules*, 2005, **38**, 10363–10372.
16. X. Hao, C. Nilsson, M. Jesberger, M. H. Stenzel, E. Malmström, T. P. Davis, E. Östmark, and C. Barner Kowollik, *Journal of Polymer Science Part A: Polymer Chemistry*, 2004, **42**, 5877–5890.
17. L. Zhang, J. Bernard, T. P. Davis, C. Barner Kowollik, and M. H. Stenzel, *Macromolecular Rapid Communications*, 2008, **29**, 123–129.
18. J. Liu, L. Tao, J. Xu, Z. Jia, C. Boyer, and T. P. Davis, *Polymer*, 2009, **50**, 4455–4463.
19. J. Liu, H. Liu, Z. Jia, V. Bulmus, and T. P. Davis, *Chem. Commun. (Camb.)*, 2008, 6582–6584.
20. A. Nese, Y. Kwak, R. Nicolaÿ, M. Barrett, and S. S. Sheiko, *Macromolecules*, 2010, **43**, 4016–4019.
21. G. Zheng and C. Pan, *Polymer*, 2005, **46**, 2802–2810.
22. C. Boyer, M. H. Stenzel, and T. P. Davis, *Journal of Polymer Science Part A: Polymer Chemistry*, 2011, **49**, 551–595.
23. D. Konkolewicz, M. J. Monteiro, and S. Perrier, *Macromolecules*, 2011, **44**, 7067–7087.
24. G. Moad, Y. K. Chong, A. Postma, E. Rizzardo, and S. H. Thang, *Polymer*, 2005, **46**, 8458–8468.
25. S. M. Henry, A. J. Convertine, D. S. W. Benoit, A. S. Hoffman, and P. S. Stayton, *Bioconjugate chemistry*, 2009, **20**, 1122–1128.
26. A. J. Convertine, D. S. W. Benoit, C. L. Duvall, A. S. Hoffman, and P. S. Stayton, *J Control Release*, 2009, **133**, 221–229.
27. D. Roy, G. Y. Berguig, B. Ghosn, D. D. Lane, S. Braswell, P. S. Stayton, and A. J. Convertine, *Polymer Chemistry*, 2014, **5**, 1791–1799.

28. D.-J. Liaw, C.-C. Huang, H.-C. Sang, and P.-L. Wu, *Polymer*, 2000, **41**, 6123–6131.
29. B. B. Lundy, A. Convertine, M. Miteva, and P. S. Stayton, 2013, **24**, 398–407.
30. N. J. Treat, D. Smith, C. Teng, J. D. Flores, B. A. Abel, A. W. York, F. Huang, and C. L. McCormick, *Macro Letters*, 2011.
31. E. Crownover, C. L. Duvall, A. CONVERTINE, A. S. Hoffman, and P. S. Stayton, *Journal of Controlled Release*, 2011, **155**, 167–174.
32. M. C. Palanca-Wessels, A. J. Convertine, R. Cutler-Strom, G. C. Booth, F. Lee, G. Y. Berguig, P. S. Stayton, and O. W. Press, *Mol. Ther.*, 2011, **19**, 1529–1537.
33. A. J. Convertine, C. Diab, M. Prieve, A. Paschal, A. S. Hoffman, P. H. Johnson, and P. S. Stayton, *Biomacromolecules*, 2010, **11**, 2904–2911.
34. C. Cheng, A. J. Convertine, P. S. Stayton, and J. D. Bryers, *Biomaterials*, 2012, **33**, 6868–6876.
35. M. J. Manganiello, C. Cheng, A. J. Convertine, J. D. Bryers, and P. S. Stayton, *Biomaterials*, 2012, **33**, 2301–2309.
25. S. M. Henry, A. J. Convertine, D. S. W. Benoit, A. S. Hoffman, and P. S. Stayton, *Bioconjugate chemistry*, 2009, **20**, 1122–1128.
26. A. J. Convertine, D. S. W. Benoit, C. L. Duvall, A. S. Hoffman, and P. S. Stayton, *J Control Release*, 2009, **133**, 221–229.
27. D. Roy, G. Y. Berguig, B. Ghosn, D. D. Lane, S. Braswell, P. S. Stayton, and A. J. Convertine, *Polymer Chemistry*, 2014, **5**, 1791–1799.

28. D.-J. Liaw, C.-C. Huang, H.-C. Sang, and P.-L. Wu, *Polymer*, 2000, **41**, 6123–6131.
29. B. B. Lundy, A. Convertine, M. Miteva, and P. S. Stayton, 2013, **24**, 398–407.

30. N. J. Treat, D. Smith, C. Teng, J. D. Flores, B. A. Abel, A. W. York, F. Huang, and C. L. McCormick, *ACS macro …*, 2011.
31. E. Crownover, C. L. Duvall, and A. CONVERTINE, *Journal of Controlled …*, 2011.

32. M. C. Palanca-Wessels, A. J. Convertine, R. Cutler-Strom, G. C. Booth, F. Lee, G. Y. Berguig, P. S. Stayton, and O. W. Press, *Mol. Ther.*, 2011, **19**, 1529–1537.
33. A. J. Convertine, C. Diab, M. Prieve, A. Paschal, A. S. Hoffman, P. H. Johnson, and P. S. Stayton, *Biomacromolecules*, 2010, **11**, 2904–2911.
34. C. Cheng, A. J. Convertine, P. S. Stayton, and J. D. Bryers, *Biomaterials*, 2012, **33**, 6868–6876.
35. M. J. Manganiello, C. Cheng, A. J. Convertine, J. D. Bryers, and P. S. Stayton, *Biomaterials*, 2012, **33**, 2301–2309.

pH-responsive endosomalytic brushes capable of spontaneously self-assembling into polymersomes were synthesized by RAFT and the intracellular delivery of antibiotic drugs was investigated.